Faraday Discussions

Investigating the Mechanism of Substrate Binding in the Solar Water Oxidation Reaction of Photosystem II Using Hyperfine Sub-level Correlation Spectroscopy

Journal:	*Faraday Discussions*
Manuscript ID	FD-ART-11-2021-000094
Article Type:	Paper
Date Submitted by the Author:	22-Nov-2021
Complete List of Authors:	Kalendra, Vidmantas; Rensselaer Polytechnic Institute, Chemistry and Chemical Biology Reiss, Krystle; Yale University, Chemistry Banerjee, Gourab; Yale University-Chemistry, Chemistry; Yale University, Chemistry Ghosh, Ipsita; Yale University-Chemistry Baldansuren, Amgalanbaatar; Rensselaer Polytechnic Institute, Chemistry and Chemical Biology Batista, Victor; Yale University, Chemistry Brudvig, Gary; Yale University-Chemistry, Lakshmi, K. V.; Rensselaer Polytechnic Institute, Chemistry and Chemical Biology

SCHOLARONE™
Manuscripts

Binding of the Substrate Analog Methanol in the Oxygen-evolving Complex of Photosystem II in the D1-N87A Genetic Variant of Cyanobacteria

Vidmantas Kalendra,[a] Krystle M. Reiss,[b] Gourab Banerjee,[b] Ipsita Ghosh,[b] Amgalanbaatar Baldansuren,[a] Victor S. Batista,[b] Gary W. Brudvig[b,*] and K. V. Lakshmi[a,*]

[a]Department of Chemistry and Chemical Biology and The Baruch '60 Center for Biochemical Solar Energy Research, Rensselaer Polytechnic Institute, Troy, New York 12180, USA

[b]Department of Chemistry, Yale University, New Haven, Connecticut 06520, USA

Corresponding Authors:

K. V. Lakshmi
Department of Chemistry and Chemical Biology
Rensselaer Polytechnic Institute
Troy, NY 12180
Phone: (518) 698 7976
E-mail: lakshk@rpi.edu

Gary W. Brudvig
Department of Chemistry
Yale University
New Haven, CT 06520
Phone: (203) 432-5202
E-mail: gary.brudvig@yale.edu

Keywords: Photosystem II, oxygen-evolving complex, oxygen evolution, S_2 state, substrate binding, methanol, EPR spectroscopy, HYSCORE spectroscopy.

Abstract.

The solar water-splitting protein complex, photosystem II (PSII), catalyzes one of the most energetically demanding reactions in nature by using light energy to drive a catalyst capable of oxidizing water. The water oxidation reaction is catalyzed at the Mn_4Ca-oxo cluster in the oxygen-evolving complex (OEC) which cycles through five light-driven S-state intermediates (S_0 - S_4). A detailed mechanism of the reaction remains elusive as it requires knowledge of the delivery and binding of substrate water in the higher S-state intermediates. In this study, we use two-dimensional (2D) hyperfine sublevel correlation spectroscopy in conjunction with quantum mechanics/molecular mechanics (QM/MM) and density functional theory (DFT) to probe the binding of the substrate analog, methanol, in the S_2 state of the D1-N87A variant of PSII from *Synechocystis* sp. PCC 6803. The results indicate that the size and specificity of the "narrow" channel is altered in D1-N87A PSII, allowing for the binding of deprotonated ^{13}C-labeled methanol at the Mn4(IV) ion of the catalytic cluster in the S_2 state. This has important implications on the mechanistic models for water oxidation in PSII.

Introduction.

The photosynthetic protein, photosystem II (PSII), catalyzes one of the most energetically demanding reactions in nature by using light energy to drive a catalyst capable of oxidizing water.[1-3] The light-driven four-electron water oxidation reaction takes place at the catalytic Mn_4Ca-oxo cluster in the oxygen-evolving complex (OEC) of PSII (**Figure 1**).[4-7] The core of the cluster is a distorted cubane comprised of three Mn (Mn1–Mn3), four O^{2-} (O1–O3 and O5), and one Ca^{2+} ion. The fourth 'dangler' Mn ion, Mn4, is connected to the cubane by two μ-O bridges, O4 and O5. The shape of the cluster resembles a distorted chair, with the cubane serving as the base and the Mn4 ion serving as the back of the chair. The distorted shape is important as its flexible nature enables the cluster to undergo structural rearrangements during the catalytic cycle. Additionally, the cluster is coordinated by six carboxylates and one histidine residue, D1-H332, which is coordinated to the Mn1 ion.[4, 8-10]

It is known that the OEC cycles through five light-driven charge-storage or S-state intermediates (S_0 - S_4) as it accumulates oxidizing equivalents to oxidize water, where S_1 is the dark state and S_4 is the final transient state that leads to O–O bond formation and oxygen evolution.[11] In recent years, conventional and time-resolved X-ray crystallography,[4, 5, 12-16] X-ray absorption fine structure (EXAFS),[7, 17-20] electron

paramagnetic resonance (EPR),[10, 21-29] FTIR[30-33] and quantum mechanics/molecular mechanics (QM/MM)[34-38] investigations have provided information on the structure and oxidation states of the metal ions in the OEC during the S-state cycle. The recent X-ray crystal structures have enabled analyses of the location and possible function of water molecules in the OEC.[4, 5, 13-16] There are four water-derived ligands coordinated to the Mn_4Ca-oxo cluster in the dark-stable S_1 state. The binding of these ligands has been studied by several methods, including magnetic resonance,[21, 39] Fourier-transform infrared spectroscopy (FTIR) spectroscopy[32, 40] and time-resolved membrane-inlet mass spectrometry (TR-MIMS).[41, 42] Based on these studies, it has been concluded that the two substrate waters are delivered to the OEC in the S_3 to S_0 and S_2 to S_3 transitions. TR-MIMS has identified two types of exchangeable substrate waters, W_f and W_s, which are in fast and slow exchange with the bulk solvent, respectively; W_s has been proposed to be a μ-oxo bridge between the Ca and Mn ion and W_f as a terminal ligand coordinated to Mn,[41, 43] although these assignments remain unclear.[44] There are additional water molecules that form an extensive hydrogen (H)-bonded network around the Mn_4Ca-oxo cluster that are positioned by amino acids that interact with the μ-oxo bridges or water ligands of the cluster, including the D1-N87, D1-S169, D1-D61, CP43-R357 and D1-H337 residues in cyanobacterial PSII.[2, 4, 5]

Although high-resolution X-ray crystallography, EXAFS and theoretical studies have provided models for the catalytic Mn_4Ca-oxo cluster, the mechanism of delivery and binding of substrate water, participation of the protein environment in substrate activation and the structure of the higher S_3 and S_4 intermediates remain heavily debated. This is important as the OEC is considered a promising blueprint for the development of artificial catalysts for water splitting that can generate clean and renewable energy from sunlight.[45-48] Currently, there is intense interest in determining the mechanism for the delivery of substrate (H_2O) and products (H^+ and O_2) to and from the Mn_4Ca-oxo cluster in the OEC during water oxidation.[49, 50] Based on computational analyses of the X-ray crystal structures, there are three putative channels that are suggested to be associated with the OEC; the “narrow”, “broad” and “large” channel.[50] The narrow and broad channels are proximal to the Mn4 ion, while the large channel is close to the Ca^{2+} ion in the Mn_4Ca-oxo cluster. The barrier for entry of water molecules in the narrow channel is suggested to be lower than that of the broad channel[50] and molecular dynamics (MD) simulations have suggested that there may be strict control of accessibility and ordered

substrate binding at the active site that is critical in regulating the complex chemistry of water oxidation.[51, 52]

Current proposals suggest that the S_2 to S_3 state transition of the OEC involves the binding of a water ligand at the Mn_4Ca-oxo cluster with the oxidation of a Mn ion.[37] However, there is considerable debate on the origin and binding mode of the water molecule. There are primarily two theoretical models proposed for the delivery of water in the S_2 to S_3 transition.[37] In the first model, a water molecule, W_X, is delivered through the narrow channel and binds to the dangler Mn4 ion through a carousel mechanism. In the second model, W_X is delivered through the large channel that is proximal to the Ca^{2+} ion and binds to the Mn1 ion through a pivot mechanism. However, recent cryo-electron microscopy studies have shown that the "large" channel is not conserved in PSII from *Synechocystis* sp. PCC 6803.[53] There is an urgent need for spectroscopic data on the function of the channels and the coordination environment of the Mn ions in order to determine the precise pathway for water delivery in the OEC. PSII is a unique case where the substrate and solvent molecules are identical and, therefore, it has been a substantial challenge to differentiate between them while probing the mechanism of substrate delivery and binding in the OEC.

There are two experimental approaches that have previously been employed to investigate the delivery of substrate: (i) to probe the water binding sites by studying indirect effects of site-directed mutagenesis of amino acid residues and (ii) to employ small molecule analogs, such as, ammonia, hydroxylamine and methanol, to probe access to the Mn_4Ca-oxo cluster in the OEC.[54-62] However, there have been few attempts to interrogate the high-resolution electronic and geometric structure of the binding of small molecule analogs associated with the various channels of site-directed variants of cyanobacterial PSII.[57] This is important as elucidation of the mechanism of water oxidation requires precise knowledge of how, when and where substrate waters bind at the Mn_4Ca-oxo cluster during the S-state cycle.

The X-ray crystal structures reveal that the asparagine-87 residue in the D1 polypeptide, D1-N87, is located in the "narrow" channel and is proximal to serine, arginine and aspartic acid residues (D1-S169, CP43-R357 and D1-D61, respectively) in PSII from *Thermosynechococcus vulcanus*.[4, 50] The D1-N87 residue has been suggested to be involved in the delivery of water molecules as well as proton transport in the OEC.[50, 63] Moreover, D1-N87 indirectly interacts with the water molecule, W_X, and is likely hydrogen (H)-bonded to the D1-S169 residue that was implicated in substrate

binding in the OEC.[64, 65] It is interesting that despite the highly-conserved sequence of the OEC across species, D1-N87 in cyanobacteria is replaced by an alanine, D1-A87, in PSII from higher plants.[50, 66] It has been suggested that an important consequence of the replacement of D1-N87 by alanine is that the shape and flexibility of the narrow channel is wider in higher plants while also removing a H-bonding residue in it.[50] Some of us have previously observed that the D1-N87A variant of *Synechocystis* PCC 6803 shows comparable S-state cycling efficiency to wild-type (WT) cyanobacterial and spinach PSII.[67] However, it displays altered chloride-binding properties and pH dependence that mimic those in spinach PSII.

Based on the location and H-bonding pattern of the D1-N87 residue, it is possible that it is also involved in the delivery of substrate water at the Mn_4Ca-oxo cluster in the S_2 to S_3 transition. More specifically, D1-N87 could regulate the size and selectivity of the putative "narrow" channel. This is important as it is plausible that this is the only channel available for water delivery and its narrow path prevents access of larger molecules that could potentially react with the OEC. Additionally, D1-N87 could participate in maintaining the well-defined H-bonding network of water molecules in and around the OEC, which regulates the entry and binding of water ligands. Previous studies involving the binding of small molecule substrate analogs in the OEC have indicated that although methanol competes with the binding of water, its binding does not inhibit oxygen evolution. More recently, Britt and coworkers have demonstrated that isotope-labeled methanol can be used as a substrate analogue to probe the binding of substrate molecules in the OEC. Using electron-spin-echo envelope modulation (ESEEM), hyperfine sublevel correlation (HYSCORE) and electron nuclear double resonance (ENDOR) spectroscopy of CD_3OH and $^{13}CH_3OH$, these studies probed the binding of methanol through the measurement of electron-nuclear hyperfine couplings of the ^2H and ^{13}C atom(s) with the paramagnetic Mn_4Ca-oxo cluster in the S_2 state of spinach PSII.[58, 59] In particular, the use of ^{13}C-methanol offered a selective probe of the location of the methyl group that allowed for the evaluation of possible methanol binding sites in spinach PSII.

In the present study, using two-dimensional (2D) hyperfine sublevel correlation (HYSCORE) spectroscopy, we present direct evidence of the binding of ^{13}C-methanol to the catalytic Mn_4Ca-oxo cluster in the S_2 state of the OEC of D1-N87A PSII from *Synechocystis* sp. PCC 6803. 2D HYSCORE spectroscopy[68] is ideally suited to probe the binding of small molecule analogs as the hyperfine interactions of magnetic nuclei

with the unpaired electron spin in the S_2 state are detected in 2D frequency space, which dramatically improves the spectral resolution. Moreover, the nuclear frequencies are correlated in the two dimensions, which crucially simplifies the analysis of experimental spectra. In conjunction with HYSCORE spectroscopy, we also employ QM/MM and density functional theory (DFT) methods to model possible binding sites of methanol and identify the most likely binding site by obtaining a best match of the experimental and calculated ^{13}C hyperfine couplings in the S_2 state of D1-N87A PSII.

Results and Discussion.

Pulsed EPR spectroscopy of ^{13}C-methanol-treated D1-N87A PSII: The S_2 state of the OEC of PSII from higher plants and cyanobacteria can be photo-accumulated by steady-state illumination at cryogenic temperatures (180 – 200 K),[69] which induces one-electron oxidation of the S_1 to S_2 state. We and others have demonstrated that the S_2 state displays distinct low- and high-spin isomers with g ~ 2.0 'multiline' and g > 4.0 EPR signals, respectively.[22, 69-71] Shown in **Figure 1SA-B** are EPR spectra of the S_2 state of wild-type (WT) and D1-N87A PSII from *Synechocystis* sp. PCC 6803 treated with 5% (v/v) ^{13}C-methanol. The S_2 state multiline EPR spectrum is centered at a g value of ~ 2.0 with an overall spectral width of 200 mT and contains 12-14 hyperfine peaks that are characteristic of the low-spin isomer of the S_2 state. The multiline signal has been shown to arise from the electron-nuclear hyperfine interactions of the effective electron spin (S = ½) with the four equivalents of ^{55}Mn nuclear spins (I = 5/2) of the Mn_4Ca-oxo cluster in the OEC. The spectra are in agreement with previously published multiline signals of the S_2 state.

In principle, the binding of ^{13}C-methanol in the OEC should lead to additional splittings in the spectrum from hyperfine interactions of the ^{13}C nuclear spin(s) (I = ½) with the paramagnetic Mn_4Ca-oxo cluster in the S_2 state. However, the ^{13}C hyperfine interactions are much weaker than the ^{55}Mn couplings in the OEC and are masked by the inhomogeneous line width of the multiline peaks. Therefore, in the present study, we probe the ^{13}C hyperfine couplings of ^{13}C-methanol-treated PSII by 2D HYSCORE spectroscopy, which has the ability to resolve the weak hyperfine interactions of the ^{13}C nuclei that are coupled to the unpaired electron spin in the S_2 state.

Shown in **Figure 2A-B** are the experimental and simulated ^{13}C HYSCORE spectra of the S_2 state of D1-N87A PSII from *Synechocystis* sp. PCC 6803 treated with 5% (v/v) ^{13}C-methanol. As can be seen in **Figure 2A**, we observe a pair of off-diagonal cross-peaks, C^I, at (5.4, 2.1) and (2.1, 5.4) MHz in the (+,+) quadrant of the HYSCORE

spectrum. The cross-peaks are centered at the ^{13}C Zeeman frequency of 3.6 MHz (at a magnetic field of 335 mT) and arise from the hyperfine interactions of the ^{13}C atom (nuclear spin, I = ½) of $^{13}CH_3OH$ that is bound to the OEC in the S_2 state. The separation between the pair of cross-peaks C^I is ~ 3.5 MHz, which is proportional to the isotropic hyperfine coupling, A_{iso}, of the ^{13}C atom of bound methanol.

We performed numerical simulations of the experimental spectrum (**Figure 2B**) to obtain a quantitative measure of the isotropic, A_{iso}, and anisotropic, T, hyperfine interactions and rhombicity parameter, δ (**Table 1**). As can be seen in **Figure 2A-B**, there is excellent agreement between the experimental and simulated line shape of the cross-peaks, C^I. The value of the A_{iso} coupling of 3.63 ± 0.15 MHz that was obtained from the numerical simulations (**Table 1**) is in agreement with the qualitative estimate predicted from the separation of the cross-peaks. The anisotropic hyperfine coupling, T, of 1.65 ± 0.11 MHz is similar in magnitude to that of the protons of a water-derived ligand coordinated to the Mn4 ion.[39] Interestingly, the cross-peaks display deviations from the anti-diagonal of the spectrum shown as a dashed red line in **Figure 2B**. It was previously noted that such cross-peak distortions in HYSCORE spectroscopy could originate from a distribution of hyperfine parameters or strain in orientationally-disordered protein samples or frozen solutions, where the hyperfine strain can be modeled using a distribution function. In order to account for the hyperfine strain observed in C^I, we employed a weighted Gaussian-type function to model the distorted line shape by assigning the center of distribution and the full-width at half maximum (FWHM) in the simulations (standard deviation, σ, of 0.3 MHz).

Additionally, the experimental spectrum in **Figure 2A** also reveals a cross-peak, C^{II}, on the diagonal which arises from very weak hyperfine couplings (A_{iso} < 0.1 MHz) of the effective electron spin (S = ½) with ambient non-bonded ^{13}C nuclei that are not directly coordinated to the Mn ions of the Mn_4Ca-oxo cluster in the S_2 state.[58, 59] Therefore, C^{II} was not included in the numerical simulations in **Figure 2B**. It is important to note that both of the cross-peaks, C^I and C^{II}, were absent in the S_2 state of untreated D1-N87A PSII (**Figure 3SA-B**) and ^{13}C-methanol-treated WT PSII from *Synechocystis* sp. PCC 6803 (**Figure 4S**), while C^I was not observed in the S_2 state of ^{13}C-methanol-treated PSII from spinach (spectrum not shown).

In order to assess the effects of methanol binding on the primary and secondary sphere of ligands to the Mn_4Ca-oxo cluster in the S_2 state, we examined the ^{14}N hyperfine interactions of ^{13}C-methanol bound D1-N87A PSII. Shown in **Figure 2SA-B**

are the experimental and simulated 2D ^{14}N HYSCORE spectra of the ^{13}C-methanol bound S_2 state of D1-N87A PSII. The ^{14}N hyperfine and quadrupolar couplings in **Table 1S** indicate that the hyperfine couplings of the nitrogen atoms are identical to those observed in the S_2 state of untreated WT PSII,[9, 10, 72] indicating that magnetic interactions with the D1-H332 and CP43-R357 residues remain unchanged in the S_2 state of ^{13}C-methanol bound D1-N87A PSII.

QM/MM and DFT studies of methanol binding in the oxygen-evolving complex: We obtained ^{13}C A_{iso} couplings of 3.63 ± 0.15 MHz and < 0.1 MHz from the 2D HYSCORE spectra of the ^{13}C-methanol bound S_2 state of D1-N87A PSII. While an A_{iso} coupling of < 0.1 MHz can be attributed to non-bonded ^{13}C nuclei, the larger ^{13}C A_{iso} of 3.63 ± 0.15 MHz suggests that methanol is directly coordinated to a paramagnetic Mn ion in the S_2 state of the OEC of D1-N87A PSII.[58] As evidenced in previous studies, direct structural assignment of the specific binding sites in the OEC based solely on the measured hyperfine parameters is limited in scope. However, it is possible to interpret the EPR parameters in conjunction with quantum mechanical models to gain insight on the binding of ligands in the OEC.[73-75]

Since the binding of methanol increases the energy separation between the S_2 state spin isomers[54, 76-78] stabilizing the S = 1/2 ground spin state of the S_2 state, we used QM/MM methods to optimize structural models of the low-spin g ~ 2.0 open cubane conformer of the Mn_4Ca-oxo cluster to evaluate the possibility of a methoxy group or methanol interacting with the Mn4(IV) or Mn1(III) ion. The QM/MM studies yielded three plausible models in which methanol binds to the cluster in the protonated or deprotonated methoxy form (**Figure 3A-C**). In the first model, Mn4-W1, a methoxy group displaces the water-derived ligand W_1 that is coordinated to the Mn4(IV) ion in the low-spin g ~ 2.0 isomer of the S_2 state, binding at a distance of 2.1 Å (**Figure 3A**). In this case, the methoxy group is accepting a hydrogen bond from the protonated D1-D61 residue. The methyl group is between the backbone of the D1-S169 residue and the water molecule, W_9, where one of the methyl hydrogen atoms donates a short (1.5 Å) hydrogen bond to W_9. In the second model Mn4-W2, a methoxide group displaces the water-derived ligand W_2, binding to Mn4(IV) at a distance of 1.8 Å, accepting a hydrogen bond from the water molecule, W_5 (**Figure 3B**). The methyl group is located less than 4 Å from the D1-V185 residue, where it is in contact with the rigid side chain of valine and one of the methyl hydrogen atoms donates a hydrogen bond (2.1 Å) to the water molecule, W_8.

In contrast to the two Mn4 models, methanol displaces D1-E189 ligand in the third model Mn1-MeOH binding to the Mn1(III) ion and donating a short (1.4 Å) hydrogen bond to the displaced D1-E189-Oε2 atom (**Figure 3C**). The Oε2 atom in turn displaces Oε1 to bind to the calcium ion of the OEC. In this case, Oε1 is no longer coordinated to a metal ion, and instead inserts itself between the waters, W_3 and W_7, disrupting the H-bonded water tetramer in the OEC. The methyl group of the methanol points towards the large channel and does not appear to form any notable interactions. We observed that the geometric parameters of the Mn and Ca ions of the Mn_4Ca-oxo cluster as well as the amino acid ligands of all three QM/MM models are consistent with the X-ray structures of PSII.[4] It is important to note that while methanol can readily access the Mn4 ion in the Mn4-W1 and Mn4-W2 models, it has very limited access to the Mn1 ion due to steric limitations of the site. Previous studies by Britt and coworkers also considered the binding of methanol either in μ-oxido positions replacing either the $O4^{2-}$ or $O5^{2-}$ ion or the W_3 water coordinated at the Ca^{2+} ion.[58] We did not consider a bridging μ-oxido as we do not observe large alterations in the ^{14}N hyperfine couplings and effective ^{55}Mn couplings. Moreover, the large ^{13}C A_{iso} value of 3.63 ± 0.15 MHz indicates that the methanol is directly coordinated to a paramagnetic Mn which limits the possibility of its binding at the Ca^{2+} ion. However, it is possible that the A_{iso} of < 0.1 MHz obtained from the experimental data represents the binding of a second methanol/methoxy group at the Ca^{2+} ion.[58, 62] As we and others have previously demonstrated, the best way to validate the QM/MM structural models of the methanol-bound S_2 state is by the prediction of the ^{13}C hyperfine interactions.[63, 73]

After validating our predictions of ^{13}C hyperfine couplings using broken-symmetry density functional theory (BS-DFT) methods to reproduce the hyperfine interactions of select computational models described by Retegan and Pantazis,[63] we calculated the ^{13}C hyperfine couplings for the three QM/MM models described above (**Table 2**) for comparison with the experimental hyperfine couplings shown in **Table 1**. We found that the calculated isotropic and anisotropic hyperfine couplings of Mn4-W2 are consistent with the results of the HYSCORE studies. As can be seen in **Table 2**, the BS-DFT calculations of the model with a methoxy group coordinated at the W_2 position of the Mn4(IV) ion yielded ^{13}C isotropic and anisotropic hyperfine couplings of 3.2 – 3.3 MHz and 1.89 – 1.90 MHz, respectively, which are close to the experimental ^{13}C A_{iso} and T value of 3.63 ± 0.15 and 1.65 ± 0.11 MHz in **Table 1**. Moreover, the ^{13}C hyperfine couplings of the Mn4-W2 model are also in the range of the previous model W2-1d[63] in a

study where the authors had selected twenty representative structures that covered a range of possibilities with respect to the interaction of methanol with the OEC. These models included structures where methanol was either protonated or deprotonated when binding as a first-sphere ligand. In general, it was found that the ^{13}C A_{iso} and T value of methoxy binding were dramatically larger (5.73 - 4.06 MHz and 1.53 - 2.96 MHz for A_{iso} and T, respectively) than the corresponding values for methanol binding, which is consistent with the larger couplings observed in the present study.

It is interesting that the results obtained with ^{13}C-methanol binding in the S_2 state of D1-N87A PSII in this study are different from those of spinach PSII. While the HYSCORE spectra of the ^{13}C-methanol bound S_2 state of D1-N87A PSII yield off-diagonal cross-peaks with a ^{13}C A_{iso} coupling of 3.63 ± 0.15 MHz, previous ^{13}C-methanol binding studies in spinach PSII displayed weak ^{13}C couplings that were not resolved by X-band HYSCORE spectroscopy.[58] Further Q-band electron nuclear double resonance (ENDOR) measurements of the samples yielded A_{iso} and T values of 0.05 ± 0.02 MHz and 0.27 ± 0.05 MHz, respectively. Based on the nearly negligible ^{13}C A_{iso} coupling, it was inferred that methanol was not binding along the Jahn−Teller axis of the Mn1(III) ion and the small anisotropic coupling T suggested that the methyl group was not part of a ligand coordinated at a Mn ion in the S_2 state.[58, 62] Isosurface plots using projection factors relevant for the low-spin S_2 state indicated that methanol could replace the W_3 water ligand coordinated at the Ca^{2+} ion of the cluster in spinach PSII. Further detailed analyses of the ^{13}C hyperfine interaction data from a series of quantum chemical models that included explicit binding of methanol at different sites indicated that it was not a direct ligand, but was likely situated at the end-point of a water channel associated with the $O4^{2-}$ bridge in the OEC of spinach PSII.[63] This observation was supported by FTIR difference and time-resolved IR[79] and proton matrix ENDOR[62] spectroscopies.

The ^{13}C A_{iso} value of 3.63 ± 0.15 MHz in the ^{13}C-methanol bound S_2 state of D1-N87A PSII is roughly comparable to the signals that were obtained from the binding of ^{13}C methanol to Mn(III)Mn(IV)salpn (where, salpn=N,N′-bis(3,5-dichlorosalicylidene)-1,3-diamino-2-hydroxypropane).[58] The cross-peaks from methanol-bound Mn(III)Mn(IV)salpn were numerically simulated by moderate A_{iso} and T couplings of 0.65 ± 0.05 MHz and 1.25 ± 0.05 MHz, respectively. In the case of Mn(III)Mn(IV)salpn, the degree of curvature of the correlation ridge was taken to be diagnostic of a large anisotropic hyperfine interaction,[80] where $T > A_{iso}$. However, we observed an opposite trend with

^{13}C-methanol binding where the A_{iso} coupling of 3.63 ± 0.15 MHz is larger than the anisotropic component of 1.65 ± 0.11 MHz.

Previous ^{13}C ENDOR measurements of the S_2 state in which either the alanine carboxylate carbons or all the carbon atoms were ^{13}C-labeled showed an A_{iso} coupling of 1.2 MHz and 1.2 - 2.0 MHz for the D1 C-terminus alanine ligand and uniformly ^{13}C-labeled ligands, respectively.[81] Subsequent studies using BS-DFT calculations suggested that symmetrically bridging carboxylate groups generally provided larger anisotropic hyperfine couplings and rhombicities than terminal or Mn–Ca bridging ligands.[82] The interpretation of the ENDOR results and computational models for the BS-DFT calculations originated prior to the high-resolution X-ray crystal structure of PSII.[4] Most recently, calculations based on models derived from the 1.9 Å resolution X-ray structure[4] indicated multiple A_{iso} couplings in the range of 1.3 – 4.3 MHz for the carboxylate ligands in the S_2 state of the OEC.[83]

By combining previous pulsed EPR and computational analyses of methanol[58, 63] and ammonia binding,[57, 61, 84-86] it was suggested that there is a unique channel active in delivery of substrate analogues to the OEC. In the literature, this channel is referred to as the “narrow” channel,[87] “E, F” channel,[88] “channel 2”[89], “O4” or “Path 3” channel.[90] Ho and Styring had initially suggested that this channel would be the most permeable to methanol.[87] Molecular dynamics simulations by Bruce and coworkers demonstrated that this channel connects the OEC directly with the lumenal surface of PSII at the cavity formed by the extrinsic PsbO and PsbU proteins, and it has the lowest free energy barrier for water permeation (peak activation energy ca. 9 kcal/mol) than all other channels.[89] Moreover, recent experiments demonstrated that NH_3 binds to the Mn4 ion in the S_2 state of the OEC.[57, 84-86] Although the conformation of the cluster is fundamentally different when NH_3 and MeOH bind to the OEC, it is appears that both analogs act as a direct ligand to the Mn4 ion. The narrow channel that is suggested as the methanol access pathway could be the same one that delivers ammonia to the Mn4 ion, supporting the notion that this is the only directly solvent-accessible manganese site of the OEC.[63] Additionally, studies of the $S_2 \rightarrow S_3$ transition and proposals for water binding in the OEC (in both the carousel and pivot mechanism),[37] have suggested that Mn4 is the only directly accessible Mn ion of the cluster and that substrate inclusion to the OEC occurs through initial binding at this site. This is in agreement with the present study where computational analysis of the ^{13}C HYSCORE experimental data indicate that a deprotonated methoxy group binds at the W_2 position at the Mn4(IV) ion in the S_2

state of D1-N87A PSII. Further studies are in progress to understand the mechanistic implications for the water oxidation reaction in the OEC.

Previous comparisons of the primary sequence of the D1 polypeptide of cyanobacteria and spinach revealed that the substitution of the D1-N87 residue by an alanine in spinach allows for the binding of methanol in the OEC. This offered a structure-based proposal for the species-dependent response to methanol. Moreover, it was found that the D1-N87A mutation made chloride binding weaker and the dissociation of chloride more facile, suggesting that replacement of D1-N87 by alanine alters the access of small molecules and ions from the lumen to the OEC.[67] Subsequently, detailed computational analyses by Pantazis and coworkers converged upon an atomistic model that was consistent with experimental observations of methanol binding in spinach PSII.[63] However, it did not directly explain why methanol binding was less pronounced in cyanobacteria. There were no species-dependent substitutions for any of the amino acid residues in the previous computational models, and hence it is improbable that fundamentally different access modes existed between species. Hence, the model must have been equally valid for both cyanobacteria and higher plants, if methanol can reach this site and adopt these positions in all organisms. The narrow channel was suggested to be the structural origin of the species-dependent response to methanol and it is proposed to act as the substrate delivery channel. Within the context of the present work, the above ^{13}C HYSCORE, QM/MM and DFT analysis establish that the substitution of the D1-N87 residue by alanine leads to the delivery and binding of methanol in the S_2 state of cyanobacterial PSII.

Conclusions.

In summary, the use of ^{13}C HYSCORE spectroscopy in conjunction with QM/MM and DFT provides evidence that ^{13}C-methanol is coordinated to the OEC in the S_2 state of D1-N87A PSII from *Synechocystis* sp. PCC 6803. Previous studies have shown that the D1-N87 residue in cyanobacterial PSII is required for efficient S-state cycling of the OEC and replacement of D1-N87 by an alanine residue alters the Cl^--binding properties such that D1-N87A PSII mimics spinach PSII. The results of the present study confirm that the size and specificity of the “narrow” channel is altered in D1-N87A PSII, allowing for the binding of deprotonated ^{13}C-labeled methanol to the Mn4 ion of the catalytic cluster, which has important implications on the mechanistic models for water oxidation in PSII.

Author Contributions. V.K., G.B., I.G. and K.V.L. conducted the experiments and analyzed the data, K.M.R. and A.B. performed QM/MM and DFT calculations, V.K., G.B., I.G., G.W.B. and K.V.L. designed the experiments and V.K., K.M.R., A.B., G.B., I.G., V.S.B., G.W.B. and K.V.L. wrote the paper.

Conflicts of Interest. The authors declare no conflicts of interests.

Acknowledgements. This work was supported by the U.S. Department of Energy, Office of Basic Energy Sciences, Photosynthetic Systems Program under the contract DE-FG02-07ER15903 (K.V.L.) and DE-FG0205ER15646 (G.W.B.). The authors would like to thank Professor R. J. Debus (University of California, Riverside) for the D1-N87A variant of *Synechocystis* sp. PCC 6803 and the Center for Computational Innovations (CCI) at Rensselaer Polytechnic Institute for computational resources.

Figures.

Figure 1. The Mn_4Ca-oxo cluster of PSII as observed in the X-ray crystal structure of PSII.[4] The core of the cluster consists of a distorted cubane comprised of three Mn, one Ca^{2+} and four μ-O^{2-} ions. A fourth dangler Mn is linked to the cubane through a μ-O^{2-} ion. There are four water-derived ligands (W_1 – W_4) to the cluster, where W_1 and W_2 are coordinated to the Mn4 ion while W_3 and W_4 are bound to the Ca^{2+} ion. Also shown are amino acid ligands to the cluster.

Figure 2. Contour-plot representation of the (+,+) quadrant of the (A) experimental and (B) overlay of the numerically simulated (pink) and experimental (purple) 2D ^{13}C HYSCORE spectrum of the ^{13}C-methanol bound S_2 state of the OEC of the D1-N87A variant of PSII from *Synechocystis* sp. PCC 6803. The spectrum was acquired at a magnetic field of 335.0 mT and temperature of 5 K. The dashed black and red lines represent the diagonal (defined by $\nu_1 = \nu_2$) and anti-diagonal (defined by $|\nu_1 \pm \nu_2| = 2_*{}^{13C}\nu$, where ${}^{13C}\nu$ is the carbon nuclear Larmor frequency), respectively.

Figure 3. QM/MM models of methanol binding at a Mn ion of the Mn_4Ca-oxo cluster in the S_2 state. The (A) Mn4-W1 model where a methoxy group replaces the water ligand W_1 at Mn4(IV) ion, (B) Mn4-W2 model where a methoxy group replaces the water ligand W_2 at Mn4(IV) ion and (C) Mn1-methanol model with methanol binding at the Mn1(III) ion. The manganese, calcium, carbon, nitrogen, oxygen and hydrogen atoms are shown in purple, yellow, grey, blue, red and white color, respectively.

Figure 1.

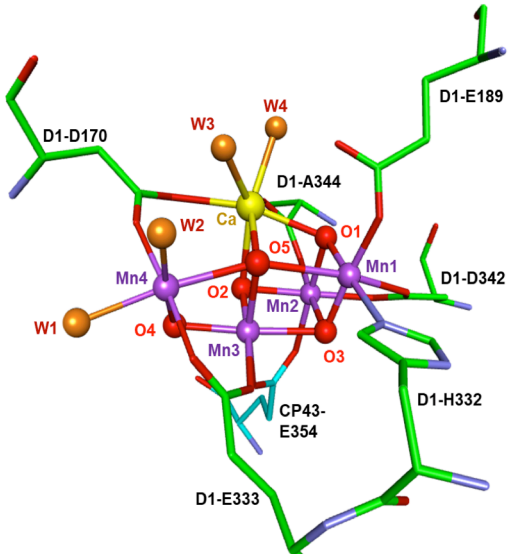
D1-D170
W3
W4
D1-E189
D1-A344
W2
Ca
O5
O1
Mn4
Mn1
D1-D342
O2
Mn2
W1
O4
Mn3
O3
D1-H332
CP43-
E354
D1-E333

Figure 2.

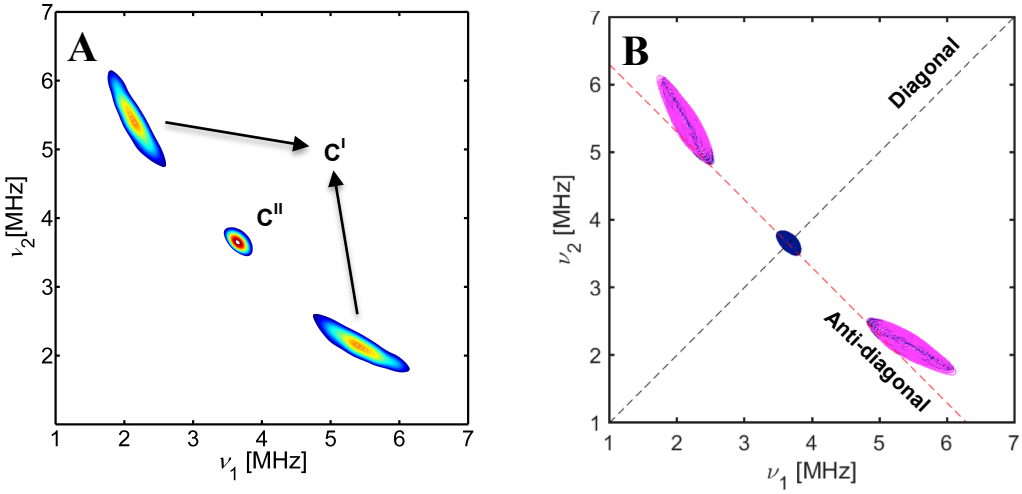

Figure 3.

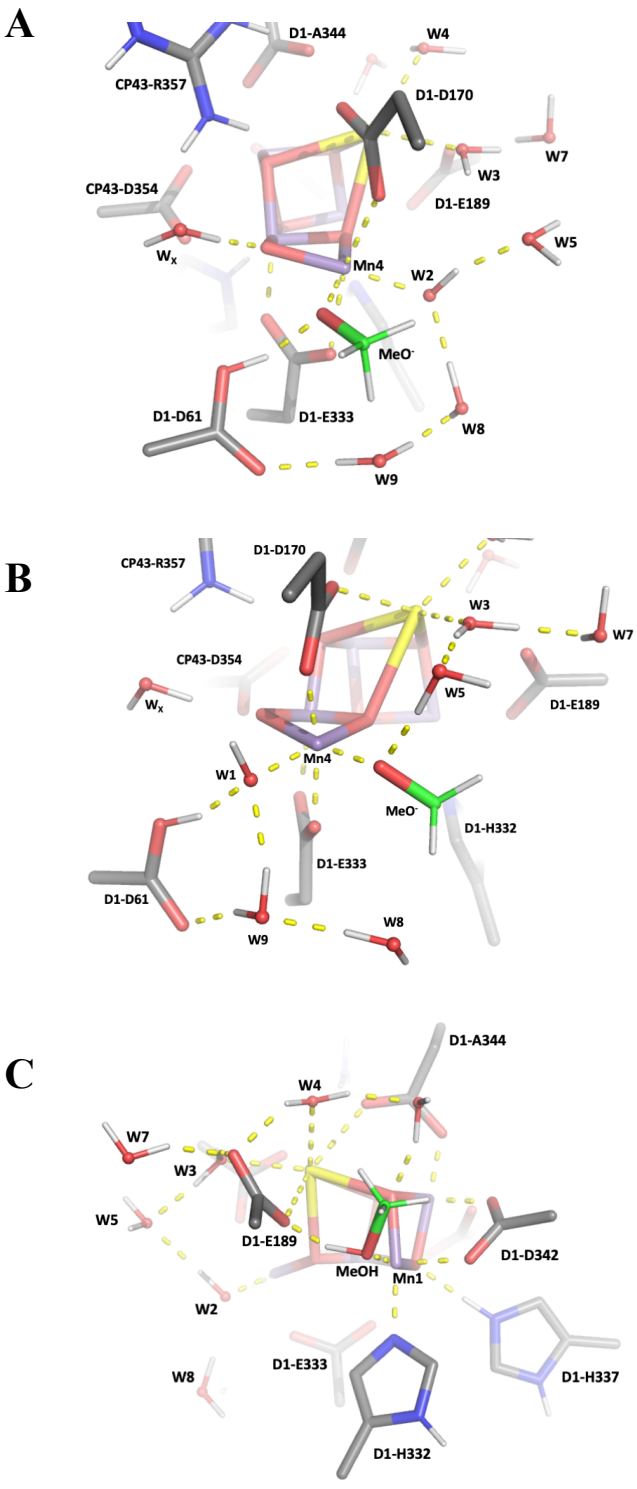
A
D1-A344
W4
CP43-R357
D1-D170
W7
W3
CP43-D354
D1-E189
W5
Wx
Mn4
W2
MeO-
D1-D61
D1-E333
W8
W9
B
CP43-R357
D1-D170
W3
W7
CP43-D354
W5
D1-E189
Wx
Mn4
W1
MeO-
D1-H332
D1-E333
D1-D61
W9
W8
C
D1-A344
W4
W7
W3
W5
D1-E189
D1-D342
MeOH
Mn1
W2
D1-E333
D1-H337
W8
D1-H332

Tables.

Table 1. Isotropic and anisotropic hyperfine parameters obtained from numerical simulations of the 2D ^{13}C HYSCORE spectrum of the S_2 state of the OEC of the ^{13}C-methanol bound D1-N87A variant of PSII from *Synechocystis* sp. PCC 6803. The hyperfine coupling constants are in units of MHz.

Nucleus	A_{iso}	T	A_x	A_y	A_z
^{13}C	3.63 ± 0.15	1.65 ± 0.11	2.4 ± 0.14	1.5 ± 0.12	7.0 ± 0.16

Table 2. Normalized ^{13}C-hyperfine constants for methanol/methoxy binding in the OEC that were calculated using a TPSSh functional with the EPR-II or ZORA/TZVP basis set. The hyperfine coupling constants are in units of MHz.

	EPR-II		ZORA/TZVP	
	A_{iso}	T	A_{iso}	T
QM/MM Model				
Mn4-W2	3.23	1.89	3.37	1.90
Mn4-W1	0.86	2.09	0.33	2.98
Mn1-MeOH	1.53	1.78	1.89	1.75

References.

[1] Vinyard, D. J., and Brudvig, G. W. (2017) Progress Toward a Molecular Mechanism of Water Oxidation in Photosystem II, *Annu. Rev. Phys. Chem. 68*, 101-116.

[2] Shen, J-R. (2015) The Structure of Photosystem II and the Mechanism of Water Oxidation in Photosynthesis, In *Annu. Rev. Plant Biol.* (Merchant, S. S., Ed.), pp 23-48.

[3] McEvoy, J. P., and Brudvig, G. W. (2006) Water-splitting Chemistry of Photosystem II, *Chem. Rev. 106*, 4455-4483.

[4] Umena, Y., Kawakami, K., Shen, J. R., and Kamiya, N. (2011) Crystal Structure of Oxygen-evolving Photosystem II at a Resolution of 1.9 Angstrom, *Nature 473*, 55-65.

[5] Suga, M., Akita, F., Sugahara, M., Kubo, M., Nakajima, Y., Nakane, T., Yamashita, K., Umena, Y., Nakabayashi, M., Yamane, T., Nakano, T., Suzuki, M., Masuda, T., Inoue, S., Kimura, T., Nomura, T., Yonekura, S., Yu, L. J., Sakamoto, T., Motomura, T., Chen, J. H., Kato, Y., Noguchi, T., Tono, K., Joti, Y., Kameshima, T., Hatsui, T., Nango, E., Tanaka, R., Naitow, H., Matsuura, Y., Yamashita, A., Yamamoto, M., Nureki, O., Yabashi, M., Ishikawa, T., Iwata, S., and Shen, J. R. (2017) Light-induced Structural Changes and the Site of O=O Bond Formation in PSII Caught by XFEL, *Nature 543* 131.

[6] Yano, J., Kern, J., Pushkar, Y., Sauer, K., Glatzel, P., Bergmann, U., Messinger, J., Zouni, A., and Yachandra, V. K. (2008) High-resolution Structure of the Photosynthetic Mn_4Ca Catalyst from X-ray Spectroscopy, *Phil. Trans. Royal Soc. B-Biol. Sci. 363*, 1139-1147.

[7] Yano, J., and Yachandra, V. K. (2008) Where Water is Oxidized to Dioxygen: Structure of the Photosynthetic Mn_4Ca Cluster From X-ray Spectroscopy, *Inorg. Chem. 47*, 1711-1726.

[8] Debus, R. J. (2008) Protein Ligation of the Photosynthetic Oxygen-evolving Center, *Coord. Chem. Rev. 252*, 244-258.

[9] Debus, R. J., Campbell, K. A., Gregor, W., Li, Z. L., Burnap, R. L., and Britt, R. D. (2001) Does Histidine 332 of the D1 Polypeptide Ligate the Manganese Cluster in Photosystem II? An Electron Spin Echo Envelope Modulation Study, *Biochemistry 40*, 3690-3699.

[10] Milikisiyants, S., Chatterjee, R., Weyers, A., Meenaghan, A., Coates, C., and Lakshmi, K. V. (2010) Ligand Environment of the S_2 State of Photosystem II: A Study of the Hyperfine Interactions of the Tetranuclear Manganese Cluster by 2D ^{14}N HYSCORE Spectroscopy, *J. Phys. Chem. B 114*, 10905-10911.

[11] Kok, B., Forbush, B., and McGloin, M. (1970) Cooperation of Charges in Photosynthetic O_2 Evolution .1. A Linear 4-Step Mechanism, *Photochem. Photobiol. 11*, 457-&.

[12] Young, I. D., Ibrahim, M., Chatterjee, R., Gul, S., Fuller, F. D., Koroidov, S., Brewster, A. S., Tran, R., Alonso-Mori, R., Kroll, T., Michels-Clark, T., Laksmono, H., Sierra, R. G., Stan, C. A., Hussein, R., Zhang, M., Douthit, L., Kubin, M., de Lichtenberg, C., Pham, L. V., Nilsson, H., Cheah, M. H., Shevela, D., Saracini, C., Bean, M. A., Seuffert, I., Sokaras, D., Weng, T. C., Pastor, E., Weninger, C., Fransson, T., Lassalle, L., Brauer, P., Aller, P., Docker, P. T., Andi, B., Orville, A. M., Glownia, J. M., Nelson, S., Sikorski, M.,

Zhu, D. L., Hunter, M. S., Lane, T. J., Aquila, A., Koglin, J. E., Robinson, J., Liang, M. N., Boutet, S., Lyubimov, A. Y., Uervirojnangkoorn, M., Moriarty, N. W., Liebschner, D., Afonine, P. V., Waterman, D. G., Evans, G., Wernet, P., Dobbek, H., Weis, W. I., Brunger, A. T., Zwart, P. H., Adams, P. D., Zouni, A., Messinger, J., Bergmann, U., Sauter, N. K., Kern, J., Yachandra, V. K., and Yano, J. (2016) Structure of Photosystem II and Substrate Binding at Room Temperature, *Nature 540*, 453.

[13] Tanaka, A., Fukushima, Y., and Kamiya, N. (2017) Two Different Structures of the Oxygen-evolving Complex in the Same Polypeptide Frameworks of Photosystem II, *J. Amer. Chem. Soc. 139*, 1718−1721.

[14] Kern, J., Chatterjee, R., Young, I. D., Fuller, F. D., Lassalle, L., Ibrahim, M., Gul, S., Fransson, T., Brewster, A. S., Alonso-Mori, R., Hussein, R., Zhang, M., Douthit, L., de Lichtenberg, C., Cheah, M. H., Shevela, D., Wersig, J., Seuffert, I., Sokaras, D., Pastor, E., Weninger, C., Kroll, T., Sierra, R. G., Aller, P., Butryn, A., Orville, A. M., Liang, M., Batyuk, A., Koglin, J. E., Carbajo, S., Boutet, S., Moriarty, N. W., Holton, J. M., Dobbek, H., Adams, P. D., Bergmann, W., Sauter, N. K., Zouni, A., Messinger, J., Yano, J., and Yachandra, V. K. (2018) Structures of the Intermediates of Kok's Photosynthetic Water Oxidation Clock, *Nature 563*, 421-425.

[15] Suga, M., Akita, F., Yamashita, K., Nakajima, Y., Ueno, G., Li, H., Yamane, T., Hirata, K., Umena, Y., Yonrkura, S., L-J., Y., Mrakami, H., Nomura, T., Kimura, T., Kubo, M., Baba, S., Kumasaka, T., Tono, K., Yabashi, M., Isobe, H., Yamaguchi, K., Yamamoto, M., Ago, H., and Shen, J.-R. (2019) An Oxyl/oxo Mechanism for Oxygen-oxygen Coupling in PSII Revealed by an X-ray free-electron Laser, *Science 366*, 334-338.

[16] Ibrahim, M., Fransson, T., Chatterjee, R., Cheah, M. H., Hussein, R., Lassalle, L., Sutherlin, K. D., Young, I. D., Fuller, F. D., Gul, S., Kim, I., Simon, P. S., de Lichtenberg, C., Chernev, P., Bogacz, I., Pham, C. C., Orville, A. M., Saichek, N., Norther, T., Batyuk, A., Carbajo, S., Alonso-Mori, R., Tono, K., Owada, S., Bhowmick, A., Bolotovsky, A. S., Adams, P. D., Sauter, N. K., Bergmann, U., Zouni, A., Messinger, J., Kern, J., Yachandra, V. K., and Yano, J. (2020) Untangling the Sequence of Events During the S_2 to S_3 Transition in Photosystem II and Implications for the Water Oxidation Mechanism, *Proc. Natl. Acad. Sci. USA 117*, 12624-12635.

[17] Sauer, K., Yano, J., and Yachandra, V. (2008) X-ray Spectroscopy of the Photosynthetic Oxygen-evolving Complex, *Coord. Chem. Rev. 252*, 318-335.

[18] Yano, J., Kern, J., Sauer, K., Latimer, M. J., Pushkar, Y., Biesiadka, J., Loll, B., Saenger, W., Messinger, J., Zouni, A., and Yachandra, V. K. (2006) Where Water is Oxidized to Dioxygen: Structure of the Photosynthetic Mn_4Ca Cluster, *Science 314*, 821-825.

[19] Dau, H., Liebisch, P., and Haumann, M. (2004) The Structure of the Manganese Complex of Photosystem II in its Dark-stable S_1 State - EXAFS Results in Relation to Recent Crystallographic Data, *Phys. Chem. Chem. Phys. 6* 4781-4792.

[20] Haumann, M., Muller, C., Liebisch, P., Iuzzolino, L., Dittmer, J., Grabolle, M., Neisius, T., Meyer-Klaucke, W., and Dau, H. (2005) Structural and Oxidation State Changes of the Photosystem II Manganese Complex in Four Transitions of the Water Oxidation Cycle (S_0 -> S_1, S_1 -> S_2, S_2 -> S_3, and S_3,S_4 -> S_0) Characterized by X-ray Absorption Spectroscopy at 20 K and Room Temperature, *Biochemistry 44*, 1894-1908.

[21] Britt, R. D., Campbell, K. A., Peloquin, J. M., Gilchrist, M. L., Aznar, C. P., Dicus, M. M., Robblee, J., and Messinger, J. (2004) Recent Pulsed EPR Studies of the Photosystem II Oxygen-evolving Complex: Implications as to Water Oxidation Mechanisms, *Biochim. Biophys. Acta-Bioenerg. 1655*, 158-171.

[22] Haddy, A. (2007) EPR Spectroscopy of the Manganese Cluster of Photosystem II, *Photosyn. Res. 92*, 357-368.

[23] Haddy, A., Lakshmi, K. V., Brudvig, G. W., and Frank, H. A. (2004) Q-band EPR of the S_2 State of Photosystem II Confirms an S = 5/2 Origin of the X-band g = 4.1 Signal, *Biophys. J. 87*, 2885-2896.

[24] Cox, N., Retegan, M., Neese, F., Pantazis, D., Boussac, A., and Lubitz, W. (2014) Electronic Structure of the Oxygen-evolving Complex in Photosystem II Prior to O-O Bond Formation, *Science 345*, 804-808.

[25] Campbell, K. A., Peloquin, J. M., Pham, D. P., Debus, R. J., and Britt, R. D. (1998) Parallel Polarization EPR Detection of an S_1 State "Multiline" EPR Signal in Photosystem II Particles from *Synechocystis* sp. PCC 6803, *J. Amer. Chem. Soc. 120*, 447-448.

[26] Lakshmi, K. V., Eaton, S. S., Eaton, G. R., Frank, H. A., and Brudvig, G. W. (1998) Analysis of Dipolar and Exchange Interactions Between Manganese and Tyrosine Z in the $S_2Y_Z^{\bullet}$ Center of Acetate-inhibited Photosystem II *via* EPR Spectral Simulations at X- and Q-Bands, *J. Phys. Chem. B 102*, 8327-8335.

[27] Lakshmi, K. V., Eaton, S. S., Eaton, G. R., and Brudvig, G. W. (1999) Orientation of the Tetranuclear Manganese Cluster and Tyrosine Z in the O_2-evolving Complex of Photosystem II: An EPR Study of the $S_2Y_Z^{\bullet}$ State in Oriented Acetate-inhibited Photosystem II Membranes, *Biochemistry 38*, 12758-12767.

[28] Messinger, J., Robblee, J. H., Yu, W. O., Sauer, K., Yachandra, V. K., and Klein, M. P. (1997) The S_0 State of the Oxygen-evolving Complex in Photosystem II is Paramagnetic: Detection of EPR Multiline Signal, *J. Amer. Chem. Soc, 119*, 11349-11350.

[29] Kulik, L. V., Epel, B., Lubitz, W., and Messinger, J. (2005) ^{55}Mn Pulse ENDOR at 34 GHz of the S_0 and S_2 States of the Oxygen-evolving Complex in Photosystem II, *J. Amer. Chem. Soc. 127*, 2392-2393.

[30] Chu, H. A., Hillier, W., Law, N. A., and Babcock, G. T. (2001) Vibrational Spectroscopy of the Oxygen-evolving Complex and of Manganese Model Compounds, *Biochim. Biophys. Acta- Bioenerg. 1503*, 69-82.

[31] Noguchi, T., and Sugiura, M. (2001) Flash-induced Fourier Transform Infrared Detection of the Structural Changes During the S-state Cycle of the Oxygen-evolving Complex in Photosystem II, *Biochemistry 40*, 1497-1502.

[32] Noguchi, T. (2008) Fourier-transform Infrared Analysis of the Photosynthetic Oxygen-evolving Center, *Coord. Chem. Rev. 252*, 336-346.

[33] Debus, R. J. (2015) FTIR Studies of Metal Ligands, Networks of Hydrogen Bonds, and Water Molecules Near the Active Site Mn_4CaO_5 Cluster in Photosystem II, *Biochim. Biophys. Acta-Bioenerg. 1847*, 19-34.

[34] Siegbahn, P. E. M. (2009) Structures and Energetics for O_2 Formation in Photosystem II, *Acc. Chem. Res. 42*, 1871-1880.

[35] Sproviero, E. M., Gascon, J. A., McEvoy, J. P., Brudvig, G. W., and Batista, V. S. (2008) Computational Studies of the O_2-evolving Complex of Photosystem II and Biomimetic Oxomanganese Complexes, *Coord. Chem. Rev. 252*, 395-415.

[36] Sproviero, E. M., Gascon, J. A., McEvoy, J. P., Brudvig, G. W., and Batista, V. S. (2007) Quantum Mechanics/Molecular Mechanics Structural Models of the Oxygen-evolving Complex of Photosystem II, *Curr. Opin. Struct. Biol. 17*, 173-180.

[37] Askerka, M., Brudvig, G. W., and Batista, V. S. (2017) The O_2-Evolving Complex of Photosystem II: Recent Insights from Quantum Mechanics/Molecular Mechanics (QM/MM), Extended X-ray Absorption Fine Structure (EXAFS), and Femtosecond X-ray Crystallography Data, *Acc. Chem. Res. 50*, 41-48.

[38] Siegbahn, P. E. M. (2017) Water Oxidation by PSII – A Quantum Chemical Approach, In *Mechanisms of Primary Energy Transduction in Biology* (Wikström, M., Ed.), The Royal Society of Chemistry.

[39] Milikisiyants, S., Chatterjee, R., Coates, C. S., Koua, F. H. M., Shen, J. R., and Lakshmi, K. V. (2012) The Structure and Activation of Substrate Water Molecules in the S_2 State of Photosystem II Studied by Hyperfine Sublevel Correlation Spectroscopy, *Energy Environ. Sci. 5*, 7747-7756.

[40] Dau, H., Noguchi, T., Messinger, J., Moran, K., and Hillier, W. (2008) FTIR Detection of Water Reactions in the Oxygen-evolving Centre of Photosystem II - Discussion, *Phil. Trans. Royal Soc. B-Biol. Sci. 363*, 1194-1195.

[41] Shevela, D., Beckmann, K., Clausen, J., Junge, W., and Messinger, J. (2011) Membrane-inlet Mass Spectrometry Reveals a High Driving Force for Oxygen Production by Photosystem II, *Proc. Natl. Acad. Sci. USA 108*, 3602-3607.

[42] Shevela, D., and Messinger, J. (2013) Studying the Oxidation of Water to Molecular Oxygen in Photosynthetic and Artificial Systems by Time-resolved Membrane-inlet Mass Spectrometry, *Front. Plant Sci. 4*, 1-9.

[43] Hillier, W., and Wydrzynski, T. T. (2000) The Affinities for the Two Substrate Water Binding Sites in the O_2-evolving Complex of Photosystem II Vary Independently During S-state Turnover, *Biochemistry 39*, 4399-4405.

[44] Huang, H.-L., and Brudvig, G. W. (2021) Kinetic Modeling of Substrate-Water Exchange in Photosystem II, *Biochim. Biophys. Adv. 1*, 100014.

[45] Young, K. J., Martini, L. A., Milot, R. L., Snoeberger, R. C., Batista, V. S., Schmuttenmaer, C. A., Crabtree, R. H., and Brudvig, G. W. (2012) Light-driven Water Oxidation for Solar Fuels, *Coord. Chem. Rev. 256*, 2503-2520.

[46] Hammarström, L., Sun, L. C., Akermark, B., and Styring, S. (1998) Artificial Photosynthesis: Towards Functional Mimics of Photosystem II?, *Biochim. Biophys, Acta-Bioenerg. 1365*, 193-199.

[47] Styring, S. (2012) Artificial Photosynthesis for Solar Fuels, *Faraday Disc. 155*, 357-376.

[48] Rivalta, I., Brudvig, G. W., and Batista, V. S. (2012) Oxomanganese Complexes for Natural and Artificial Photosynthesis, *Curr. Opin. Chem. Biol. 16*, 11-18.

[49] Linke, K., and Ho, F. M. (2014) Water in Photosystem II: Structural, Functional and Mechanistic Considerations, *Biochim. Biophys. Acta-Bioenerg. 1837*, 14-32.

[50] Vogt, L., Vinyard, D. J., Khan, S., and Brudvig, G. W. (2015) Oxygen-evolving Complex of Photosystem II: An Analysis of Second-shell Residues and Hydrogen-bonding Networks, *Curr. Opin. Chem. Biol. 25*, 152-158.

[51] Ishikita, H., Saenger, W., Loll, B., Biesiadka, J., and Knapp, E. W. (2006) Energetics of a Possible Proton Exit Pathway for Water Oxidation in Photosystem II, *Biochemistry 45*, 2063-2071.

[52] Gabdulkhakov, A. G., Kljashtorny, V. G., and Dontsova, M. V. (2015) Molecular Dynamics Studies of Pathways of Water Movement in Cyanobacterial Photosystem II, *Cryst. Reports 60*, 83-89.

[53] Gisriel, C. J., Wang, J., Liu, J., Flesher, D. A., Reiss, K. M., Huang, H.-L., Yang, K. R., Armstrong, W. H., Gunner, M. R., Batista, V. S., Debus, R. J., and Brudvig, G. W. (2021) High-resolution Cryo-EM Structure of Photosystem II from the Mesophilic Cyanobacterium, *Synechocystis* sp. PCC 6803, *Proc. Natl. Acad. Sci. USA 118*, Manuscript in Press.

[54] Deak, Z., Peterson, S., Geijer, P., Ahrling, K. A., and Styring, S. (1999) Methanol Modification of the Electron Paramagnetic Resonance Signals from the S_0 and S_2 States of the Water-oxidizing Complex of Photosystem II, *Biochim. Biophys. Acta-Bioenerg. 1412*, 240-249.

[55] Britt, R. D., Zimmermann, J. L., Sauer, K., and Klein, M. P. (1989) The State of Manganese Iin the Photosynthetic Apparatus .10. Ammonia Binds to the Catalystic Mn of the Oxygen-evolving Complex of Photosystem II - Evidence by Electron-spin-echo Envelope Modulation Spectroscopy, *J. Amer. Chem. Soc. 111*, 3522-3532.

[56] Beck, W. F., de Paula, J. C., and Brudvig, G. W. (1986) Ammonia Binds to the Manganese Site of the O_2-evolving Complex of Photosystem II in the S_2 State., *J. Amer. Chem. Soc. 108*, 4018-4022.

[57] Oyala, P. H., Stich, T. A., Debus, R. J., and Britt, R. D. (2015) Ammonia Binds to the Dangler Manganese of the Photosystem II Oxygen-evolving Complex, *J. Amer. Chem. Soc. 137*, 8829-8837.

[58] Oyala, P. H., Stich, T. A., Stull, J. A., Yu, F., Pecoraro, V. L., and Britt, R. D. (2014) Pulse Electron Paramagnetic Resonance Studies of the Interaction of Methanol with the S_2 State of the Mn_4O_5Ca Cluster of Photosystem II, *Biochemistry 53*, 7914−7928.

[59] Force, D. A., Randall, D. W., Lorigan, G. A., Clemens, K. L., and Britt, R. D. (1998) ESEEM Studies of Alcohol Binding to the Manganese Cluster of the Oxygen Evolving Complex of Photosystem II, *J. Amer. Chem. Soc. 120*, 13321-13333.

[60] Beck, W. F., and Brudvig, G. W. (1987) Reactions of Hydroxylamine with the Electron-Donor Side of Photosystem II, *Biochemistry 26*, 8285-8295.

[61] Marchiori, D. A., Oyala, P. H., Debus, R. J., Stich, T. A., and Britt, R. D. (2018) Structural Effects of Ammonia Binding to the Mn_4CaO_5 Cluster of Photosystem II, *J. Phys. Chem. B 122*, 1588.

[62] Nagashima, H., and Mino, H. (2017) Location of Methanol on the S_2 State Mn Cluster in Photosystem II Studied by Proton Matrix Electron Nuclear Double Resonance, *J. Phys. Chem. Lett. 8*, 621–625.

[63] Retegan, M., and Pantazis, D. A. (2016) Interaction of Methanol with the Oxygen-evolving Complex: Atomistic Models, Channel Identification, Species Dependence, and Mechanistic Implications, *Chem. Sci. 216*, 6463–6476.

[64] Ghosh, I., Banerjee, G., Reiss, K., Kim, C. J., Debus, R. J., Batista, V. S., and Brudvig, G. W. (2020) D1-S169A Substitution of Photosystem II Reveals a Novel S_2 state Structure, *Biochim. Biophys. Acta- Bioenerg. 1861*, 148301.

[65] Ghosh, I., Banerjee, G., Kim, C. J., Reiss, K., Batista, V. S., Debus, R. J., and Brudvig, G. W. (2019) D1-S169A Substitution of Photosystem II Perturbs Water Oxidation, *Biochemistry 58*, 1379-1387.

[66] Retegan, M., and Pantazis, D. A. (2017) Differences in the Active Site of Water Oxidation among Photosynthetic Organisms, *J. Amer. Chem. Soc. 139* 14340-14343.

[67] Banerjee, G., Ghosh, I., Kim, C. J., Debus, R. J., and Briudvig, G. W. (2018) Substitution of the D1-Asn87 Site in Photosystem II of Cyanobacteria Mimics the Chloride-binding Characteristics of Spinach Photosystem II, *J. Biol. Chem. 293*, 2487–2497.

[68] Höfer, P., Grupp, A., Nebenführ, H., and Mehring, M. M. (1986) Hyperfine Sublevel Correlation (HYSCORE) Spectroscopy: A 2D ESR Investigation of the Squaric Acid Radical, *Chem. Phys. Lett. 132*, 279–282.

[69] Brudvig, G. W., Casey, J. L., and Sauer, K. (1983) The Effect of Temperature on the Formation and Decay of the Multiline Electron Paramagnetic Resonance Signal Species Associated With Photosynthetic Oxygen Evolution, *Biochim. Biophys. Acta 723*, 366-371.

[70] Dismukes, G. C., and Siderer, Y. (1981) Intermediates of a Polynuclear Manganese Center Involved in Photosynthetic Oxidation of Water, *Proc. Natl. Acad. Sci. USA-Biol. Sci. 78*, 274-278.

[71] Britt, R. D., Lorigan, G. A., Sauer, K., Klein, M. P., and Zimmermann, J. L. (1992) The g = 2 Multiline EPR Signal of the S_2 State of the Photosynthetic Oxygen-evolving Complex Originates from a Ground Spin State, *Biochim. Biophys. Acta 1140*, 95-101.

[72] Stich, T. A., Yeagle, G. J., Service, R. J., Debus, R. J., and Britt, R. D. (2011) Ligation of D1-His332 and D1-Asp170 to the Manganese Cluster of Photosystem II from Synechocystis Assessed by Multifrequency Pulse EPR Spectroscopy, *Biochemistry 50*, 7390-7404.

[73] Yang, K., Lakshmi, K. V., Brudvig, G. W., and Batista, V. S. (2021) Is Deprotonation of the Oxygen-Evolving Complex of Photosystem II during the $S_1 \rightarrow S_2$ Transition Suppressed by Proton Quantum Delocalization?, *J. Amer. Chem. Soc. 143*, 8324-8332.

[74] Pantazis, D. A., Ames, W., Cox, N., Lubitz, W., and Neese, F. (2012) Two Interconvertible Structures that Explain the Spectroscopic Properties of the Oxygen-Evolving Complex of Photosystem II in the S_2 State, *Angew. Chem.-Intl. Ed. 51*, 9935-9940.

[75] Pantazis, D. A., Orio, M., Petrenko, T., Zein, S., Lubitz, W., Messinger, J., and Neese, F. (2009) Structure of the Oxygen-evolving Complex of Photosystem II: Information on the S_2 State Through Quantum Chemical Calculation of Its Magnetic Properties, *Phys. Chem. Chem. Phys. 11*, 6788–6798.

[76] Su, J.-H., Cox, N., Ames, W., Pantazis, D. A., Rapatskiy, L., Lohmiller, T., Kulik, L. V., Dorlet, P., Rutherford, A. W., Neese, F., Boussac, A., Lubitz, W., and Messinger, J. (2011) The Electronic Structures of the S_2 States of the Oxygen-evolving Complexes of Photosystem II in Plants and Cyanobacteria in the Presence and Absence of Methanol, *Biochim. Biophys. Acta-Bioenerg. 1807*, 829–840.

[77] Su, J.-H., Havelius, K. G. V., Mamedov, F., Ho, F. M., and Styring, S. (2006) Split EPR Signals from Photosystem II Are Modified by Methanol, Reflecting S State-Dependent Binding and Alterations in the Magnetic Coupling in the $CaMn_4$ Cluster, *Biochemistry 45*, 7617–7627.

[78] Yamauchi, T., Mino, H., Matsukawa, T., Kawamori, A., and Ono, T.-a. (1997) Parallel Polarization Electron Paramagnetic Resonance Studies of the S_1 State Manganese Cluster in the Photosynthetic Oxygen-evolving System, *Biochemistry 36*, 7520–7526.

[79] Yata, H., and Noguchi, T. (2018) Mechanism of Methanol Inhibition of Photosynthetic Water Oxidation As Studied by Fourier Transform Infrared Difference and Time-resolved Infrared Spectroscopies, *Biochemistry 57*, 4803–4815.

[80] Schweiger, A., and Jeschke, G. (2001) *Principles of Pulse Electron Paramagnetic Resonance*, Oxford University Press.

[81] Stull, J. A., Stich, T. A., Service, R. J., Debus, R. J., Mandal, S. K., Armstrong, W. H., and Britt, R. D. (2010) ^{13}C ENDOR Reveals That the D1 Polypeptide C-terminus is Directly Bound to Mn in the Photosystem II Oxygen-evolving Complex, *J. Amer. Chem. Soc. 132*, 446.

[82] Schinzel, S., Schraut, J., Arbuznikov, A. V., Siegbahn, P. E. M., and Kaupp, M. (2010) Density Functional Calculations of ^{55}Mn, ^{14}N and ^{13}C Electron Paramagnetic Resonance Parameters Support an Energetically Feasible Model System for the S_2 State of the Oxygen-evolving Complex of Photosystem II, *Chem. Eur. J. 16*, 10424 – 10438.

[83] Beal, N. J., Corry, T. A., and O'Malley, P. J. (2017) Comparison between Experimental and Broken Symmetry DensityFunctional Theory (BS-DFT) Calculated Electron ParamagneticResonance (EPR) Parameters of the S_2 State of the Oxygen-evolving Complex of Photosystem II in Its Native (Calcium) and Strontium-substituted Form, *J. Phys. Chem. B 121*, 11273−11283.

[84] Lohmiller, T., Krewald, V., Navarro, M. P., Retegan, M., Rapatskiy, L., Nowaczyk, M. M., Boussac, A., Neese, F., Lubitz, W., Pantazis, D. A., and Cox, N. (2014) Structure, Ligands and Substrate Coordination of the Oxygen-evolving Complex of Photosystem II in the S_2 State: A Combined EPR and DFT Study, *Phys. Chem. Chem. Phys. 16*, 11877–11892.

[85] Schraut, J., and Kaupp, M. (2014) On Ammonia Binding to the Oxygen-Evolving Complex of Photosystem II: A Quantum Chemical Study, *Chem.–Eur. J. 20*, 7300–7308.

[86] Navarro, M. P., Ames, W. M., Nilsson, H., Lohmiller, T., Pantazis, D. A., Rapatskiy, L., Nowaczyk, M. M., Neese, F., Boussac, A., Messinger, J., Lubitz, W., and Cox, N. (2013) Ammonia Binding to the Oxygen-evolving Complex of Photosystem II Identifies the Solvent-Exchangeable Oxygen Bridge (μ-oxo) of the Manganese Tetramer, *Proc. Natl. Acad. Sci. USA 110*, 15561-15566.

[87] Ho, F. M., and Styring, S. (2008) Access Channels and Methanol Binding Site to the $CaMn_4$ Cluster in Photosystem II Based on Solvent Accessibility Simulations, With Implications for Substrate Water Access, *Biochim. Biophys. Acta-Bioenerg. 1777*, 140-153.

[88] Gabdulkhakov, A., Guskov, A., Broser, M., Kern, J., Müh, F., Saenger, W., and Zouni, A. (2009) Probing the Accessibility of the Mn_4Ca Cluster in Photosystem II: Channels Calculation, Noble Gas Derivatization, and Cocrystallization With DMSO, *Structure 17*, 1223−1234.

[89] Vassiliev, S., Zaraiskaya, T., and Bruce, D. (2012) Exploring the Energetics of Water permeation in Photosystem II by Multiple Steered Molecular Dynamics Simulations, *Biochim. Biophys. Acta 1817*, 1671−1678.

[90] Ogata, K., Yuki, T., Hatakeyama, M., Uchida, W., and Nakamura, S. (2013) All-atom Molecular Dynamics Simulation of Photosystem II Embedded in Thylakoid Membranes, *J. Amer. Chem. Soc. 135*, 15670−15673.